

Synthesis and Structures of $\text{Mo}_3\text{Se}_7\text{Te}_2\text{Br}_{10}$, $\text{Mo}_3\text{Se}_7\text{TeI}_6$, and $\text{Mo}_6\text{Te}_{21}\text{I}_{22}$ Containing TeX_3^- ($X = \text{Br}, \text{I}$) Ligands Coordinated to a Triangular Cluster Core[†]

Maxim N. Sokolov,* Artem L. Gushchin, Pavel A. Abramov, Alexander V. Virovets, Eugenia V. Peresypkina, and Vladimir P. Fedin

Nikolaev Institute of Inorganic Chemistry, Siberian Branch of the Russian Academy of Sciences, Prospect Lavrentieva 3, Novosibirsk 630090, Russia

Received January 11, 2007

New ternary and quaternary molybdenum cluster chalcogenides were obtained by high-temperature reactions between Mo, chalcogens, and halogens in evacuated ampules. The crystal structures of $[\text{Mo}_3\text{Se}_7(\text{TeBr}_3)\text{Br}_2]_2[\text{Te}_2\text{Br}_{10}]$ (**1**), $[\text{Mo}_3\text{Se}_7(\text{TeI}_3)_2]\text{I}$ (**2**), and $[\text{Mo}_3\text{Te}_7(\text{TeI}_3)_3]_2(\text{I})$ (**3**) were determined by single-crystal X-ray diffraction. The structures of **1** and **2** consist of positively charged zigzag chains $[\text{Mo}_3\text{Se}_7(\text{TeX}_3)\text{X}_{4/2}]$ ($X = \text{Br}, \text{I}$), with $\text{Te}_2\text{Br}_{10}^{2-}$ and I^- , respectively, as counterions. The TeI_3^- and TeBr_3^- ions function as bidentate ligands in **1** and **2**. In **3**, TeI_3^- is not coordinated to the metal but acts as a counterion to the $[\text{Mo}_3\text{Te}_7(\text{TeI}_3)_3]^+$ cluster cation.

Introduction

A family of triangular chalcogen-rich clusters of Mo and W, $\text{M}_3(\mu_3\text{-Q})(\mu\text{-Q}_2)_3^{4+}$ ($M = \text{Mo}, \text{W}; Q = \text{S}, \text{Se}, \text{Te}$), has gradually emerged from the research over the last 30 years.¹ The cluster core, $\text{M}_3(\mu_3\text{-Q})(\mu\text{-Q}_2)_3^{4+}$ (or simple $\text{M}_3\text{Q}_7^{4+}$), features extraordinary stability combined with interesting reactivity patterns, which enabled the stabilization of new ligands, such as SeS^{2-} ,² TeSe^{2-} ,³ and TeS^{2-} ,⁴ for the first time, as well as observation of a new type of coordination isomerism;⁵ it also features a strong tendency to exhibit specific, directed, nonvalent interactions through the $\mu\text{-Q}_2$ ligands.^{6,7} Moreover, these clusters can be easily transformed into incomplete cuboidal clusters and their heterometal cuboidal

derivatives, $\text{M}_3(\mu_3\text{-Q})(\mu\text{-Q})_3^{4+}$ and $\text{M}_3\text{M}'(\mu_3\text{-Q})_4^{n+}$, respectively,^{1,8} whose unique reactivity and catalytic properties are now under study in a number of research groups.^{9–11} A complex of $\text{Mo}_3\text{S}_7^{4+}$ with 1,3-dithia-2-thione-4,5-dithiolate was recently shown to be a single-component molecular conductor.¹² Among the most popular lead-in materials into this rich chemistry are the polymeric chalcogenides $\text{M}_3\text{Q}_7\text{X}_4$ ($X = \text{Cl}, \text{Br}, \text{I}$). They can easily be prepared, most typically from the stoichiometric mixture of the elements, and currently they are known almost for all combinations of M, Q, and X: $\text{Mo}_3\text{Q}_7\text{Cl}_4$ ($Q = \text{S}, \text{Se}$);¹³ $\text{W}_3\text{S}_7\text{Cl}_4$ ¹⁴ and $\text{M}_3\text{Q}_7\text{Br}_4$ ($M = \text{Mo}, \text{W}; Q = \text{S}, \text{Se}$);^{13d,15,16} $\text{Mo}_3\text{Q}_7\text{I}_4$ ($Q = \text{S}, \text{Se}$),¹⁷ and poorly characterized $\text{Mo}_3\text{Te}_7\text{I}_4$, $\text{W}_3\text{Te}_7\text{I}_4$, and W_3Te_7

* To whom correspondence should be addressed. E-mail: caesar@che.nsk.su.

[†] This work is dedicated to Professor S. P. Gubin on the occasion of his 70th birthday.

- (1) Sokolov, M. N.; Fedin, V. P.; Sykes, A. G. *In Comprehensive Coordination Chemistry II*; McCleverty, J. A., Meyer, T. J., Eds.; Elsevier: New York, 2003; Vol. 4, p 761.
- (2) Fedin, V. P.; Mironov, Yu. V.; Sokolov, M. N.; Kolesov, B. A.; Fedorov, V. Ye.; Yufit, D. S.; Struchkov, Yu. T. *Inorg. Chim. Acta* **1990**, *174*, 275.
- (3) Sokolov, M. N.; Abramov, P. A.; Gushchin, A.; Kalinina, I.; Naumov, D. Yu.; Virovets, A. V.; Peresypkina, E.; Vicent, C.; Llusar, R.; Fedin, V. P. *Inorg. Chem.* **2005**, *44*, 8116.
- (4) Sokolov, M. N.; Gushchin, A. G.; Fedin, V. P., to be published.
- (5) Hernandez-Molina, R.; Sokolov, M.; Nuñez, P.; Mederos, A. *J. Chem. Soc., Dalton Trans.* **2002**, 1072.
- (6) Mayor-Lopez, M.; Weber, M.; Hegetschweiler, K.; Meienberger, M. D.; Jobo, F.; Leoni, S.; Nesper, R.; Reiss, G. J.; Frank, W.; Kolesov, B.; Fedin, V.; Fedorov, V. *Inorg. Chem.* **1998**, *37*, 2633.

- (7) (a) Virovets, A. V.; Podberezskaya, N. V. *Zh. Struct. Khim.* **1993**, *34*, 150. (b) Virovets, A. V.; Gushchin, A. L.; Abramov, P. A.; Alferova, N. I.; Sokolov, M. N.; Fedin, V. P. *Zh. Struct. Khim.* **2006**, *47*, 332.
- (8) Fedin, V. P.; Sykes, A. G. *Inorg. Synth.* **2002**, *33*, 162.
- (9) Sokolov, M. N.; Hernandez-Molina, R.; Clegg, W.; Fedin, V. P.; Mederos, A. *Chem. Commun.* **2003**, 140.
- (10) (a) Wakabayashi, T.; Ishii, Y.; Murata, T.; Mizobe, Y.; Hidai, M. *Tetrahedron Lett.* **1995**, *36*, 5585. (b) Wakabayashi, T.; Ishii, Y.; Ishikawa, K.; Hidai, M. *Angew. Chem., Int. Ed. Engl.* **1996**, *35*, 2123.
- (11) Feliz, M.; Guillamon, E.; Llusar, R.; Vicent, C.; Stiriba, S.; Perez-Prieto, J.; Barberis, M. *Chem.—Eur. J.* **2006**, *12*, 1486.
- (12) Llusar, R.; Uriel, S.; Vicent, C.; Clemente-Juan, J. M.; Coronado, E.; Gomez-Garcia, C. J.; Braida, B.; Canadell, E. *J. Am. Chem. Soc.* **2004**, *126*, 12076.
- (13) (a) Opalovskii, A. A.; Fedorov, V. E.; Khaldoyanidi, K. A. *Dokl. Akad. Nauk SSSR* **1968**, *82*, 1096. (b) Marcoll, J.; Rabenau Mootz, D.; Wunderlich, H. *Rev. Chim. Miner.* **1974**, *11*, 607. (c) Mazhara, A. P.; Opalovskii, A. A.; Fedorov, V. E.; Kirik, S. D. *Zh. Neorg. Khim.* **1977**, *22*, 1827. (d) Fedorov, V. E.; Mironov, Yu. V.; Kuzmina, O. A.; Fedin, V. P. *Zh. Neorg. Khim.* **1986**, *31*, 2476.

Br₄.^{3,18} They are usually obtained as solids of poor crystallinity, and so far only crystal structures for Mo₃S₇Cl₄ and W₃S₇Br₄ have been established from X-ray diffraction data on single crystals.^{13b,16} Both compounds were found to be built of zigzag chains ${}_4[M_3Q_7X_2X_{4/2}]$ and are one-dimensional coordination polymers. The rest of the ternaries listed above are simply assumed to have the same structure. This assumption is based on the stoichiometry, vibration spectroscopy, and (chiefly) reactivity. It was shown for the Mo–Te–I system that, in the presence of an excess of Te and I₂, the polymeric structure gives way to discrete ionic pairs [Mo₃Te₇(TeI₃)₃]I (according to X-ray data) in a new phase of the overall stoichiometry Mo₃Te₁₀I₁₀.¹⁹ In the present work we report the preparation and crystal structures of new molybdenum Mo₃Se₇⁴⁺ and Mo₃Te₇⁴⁺ clusters from the Mo–Se–Te–X (X = Br, I) and Mo–Te–I systems.

Experimental Section

Materials and Methods. High-purity Mo, Se, and Te powders were used. Br₂ was dried over P₄O₁₀ and distilled. I₂ was sublimed before use. Raman spectra were obtained on a Triplimate SPEX spectrometer using a 632.8 nm line of a He–Ne laser for excitation. X-ray powder diffraction data were obtained on a PW1700 automated powder diffractometer (Cu K α radiation).

Synthesis and Characterization. [Mo₃Se₇(TeBr₃)Br₂]₂[Te₂Br₁₀] (1). Mo powder (0.58 g, 6.0 mmol), Se (1.11 g, 13.9 mmol), Te (0.51 g, 4.0 mmol), and Br₂ (1.60 g, 10.0 mmol) were loaded in a glass ampule, which was evacuated after three cycles of freezing/thawing by liquid N₂, flame-sealed, and heated at 200 °C (1 day) and at 350 °C (6 days) in a furnace with a small natural temperature gradient. Most of **1** remained in the hotter zone as a pure single phase (powder diffraction). Yield of the product (in the hotter zone): 3.2 g (84%). Element ratio: Mo_{3.0}/Se_{7.1}Te_{1.9}/Br_{9.8} (energy-dispersive X-ray analysis, EDAX). Raman spectroscopy (cm⁻¹): 340 w, 318 w, 290 w, 270 w, 244 s, 237 m, 224 s, 126 w, 107 w, 76 m, 49 m.

[Mo₃Se₇(TeI₃)I]₂ (2). Mo powder (0.19 g, 2.0 mmol), Se (0.36 g, 4.6 mmol), Te (0.084 g, 0.66 mmol), and I₂ (0.50 g, 2.0 mmol) were loaded in a glass ampule, which was evacuated after three cycles of freezing/thawing by liquid N₂, flame-sealed, and heated at 350 °C (3 days) in a furnace with a small natural temperature gradient. Most of **2** remained in the hotter zone as a pure single phase (powder diffraction). Yield of the product (in the hotter zone): 1.0 g (88%). Element ratio: Mo_{3.0}/Se_{7.1}Te_{0.9}I_{5.9} (EDAX). Raman spectroscopy (cm⁻¹): 268 w, 173 w, 140 m, 122 s, 94 w.

- (14) (a) Saito, T.; Yoshikawa, A.; Yamagata, T.; Imoto, H.; Unoura, K. *Inorg. Chem.* **1989**, *28*, 3588. (b) Fedin, V. P.; Sokolov, M. N.; Gerasko, O. A.; Kolesov, B. A.; Fedorov, V. E.; Mironov, A. V.; Yufit, D. S.; Slovohtov, Yu. L.; Struchkov, Yu. T. *Inorg. Chim. Acta* **1990**, *175*, 217.
- (15) (a) Opalovskii, A. A.; Fedorov, V. E.; Mazhara, A. P.; Cheremisina, I. M. *Zh. Neorg. Khim.* **1972**, *17*, 2876. (b) Fedorov, V. E.; Evstafiev, V. K.; Mazhara, A. P. *Izv. Sib. Otd. AN SSSR, Ser. Khim.* **1981**, *4* (2), 47. (c) Fedin, V. P.; Sokolov, M. N.; Gerasko, O. A.; Virovets, A. V.; Podbereskaya, N. V.; Fedorov, Ye, V. *Inorg. Chim. Acta* **1991**, *187*, 81.
- (16) Cotton, F. A.; Kibala, P. A.; Matucz, M.; McCaleb, C. S.; Sangor, R. B. W. *Inorg. Chem.* **1989**, *28*, 2623.
- (17) Fedorov, V. E.; Mazhara, A. P.; Evstafiev, V. K.; Kirik, S. D. *Izv. Sib. Otd. AN SSSR, Ser. Khim.* **1978**, *14*, 56.
- (18) (a) Fedin, V. P.; Imoto, H.; Saito, T.; McFarlane, W.; Sykes, A. G. *Inorg. Chem.* **1995**, *34*, 5097. (b) Chen, H.; Lin, X.; Chi, L.; Lu, C.; Zhuang, H.; Huang, J. *Inorg. Chem. Commun.* **2000**, *3*, 331.
- (19) Fedin, V. P.; Imoto, H.; Saito, T. *J. Chem. Soc., Chem. Commun.* **1995**, 1559.

Table 1. Selected Crystal and Refinement Data for **1–3**

	1	2	3
formula	Br ₂₀ Mo ₆ Se ₁₄ Te ₄	I ₆ Mo ₃ Se ₇ Te	I ₂₂ Mo ₆ Te ₂₁
fw	3789.68	1729.54	6035.88
space group, Z	P $\bar{1}$, 1	P2 ₁ /n, 4	P $\bar{1}$, 1
a, Å	10.1638(4)	10.4969(17)	11.2148(6)
b, Å	11.0421(4)	13.029(2)	11.6550(6)
c, Å	12.5200(4)	16.567(2)	16.6798(13)
α , deg	85.461(2)	90	92.124(3)
β , deg	85.529(2)	102.921(5)	102.223(2)
γ , deg	76.410(2)	90	117.427(2)
V, Å ³	1358.94(8)	2208.3(6)	1868.4(2)
μ (Mo K α), mm ⁻¹	27.535	22.879	18.113
d _{calc} , g cm ⁻³	4.631	5.202	5.374
2 θ _{max} , deg	50	50	50
no. of rflns	5420	3891	8183
final R1, wR2	0.0420, 0.1022	0.0643, 0.1445	0.0463, 0.0960
[I > 2 σ (I)] ^a			

$$^a R1 = \sum ||F_o| - |F_c|| / \sum |F_o|; wR2 = \{ \sum [w(F_o^2 - F_c^2)^2] / \sum [w(F_o^2)^2] \}^{1/2}, w = \sigma_F^{-2}.$$

[Mo₃Te₇(TeI₃)₃]₂(I)(TeI₃) (3). Mo powder (0.25 g, 2.6 mmol), MoO₃ (0.047 g, 0.33 mmol), Te (0.76 g, 6.0 mmol), and I₂ (0.50 g, 2.0 mmol) were loaded in a glass ampule, which was evacuated after three cycles of freezing/thawing by liquid N₂, flame-sealed, and heated at 400 °C (4 days) in a furnace with a small natural temperature gradient. The composition and structure of **3** have been determined by single-crystal X-ray diffraction.

X-ray Structure Determinations. Crystallographic data and structure refinement details are given in Table 1. Diffraction data for all compounds were collected on a Bruker X8APEX CCD diffractometer with Mo K α radiation ($\lambda = 0.71073$ Å) using ϕ and ω scans of narrow (0.5°) frames. All structures were solved by direct methods and refined by full-matrix least-squares treatment against $|F|^2$ in anisotropic approximation using the *SHELXTL* program set.²⁰ Absorption corrections were applied empirically using the *SADABS* program.²¹ Further details may be obtained from the Fachinformationszentrum Karlsruhe, 76344 Eggenstein-Leopoldshafen, Germany (fax, (+49) 7247-808-666; e-mail, crysdata@fiz-karlsruhe.de) on quoting the depository numbers 417394–417396. Intermolecular interactions in the crystal and topologies of molecular packing were analyzed with the program set for multipurpose crystallochemical analysis *TOPOS 4.0 Professional*.²²

Results and Discussion

1 and **2** are obtained by heating the elements in the required stoichiometric ratio at 350 °C. Compound **3** was prepared by the reaction of Mo, MoO₃, Te, and I₂ in a 8:1:18:6 ratio at 400 °C. The syntheses were carried out in evacuated glass ampules for several days. The ampules were cooled at 4 °C/h to promote crystal growth. Some single crystals of **3** were obtained together with Mo₃Te₁₀I₁₀¹⁹ and TeI₂₃ identified by unit cell parameters.

The structures of **1–3** have been determined by single-crystal X-ray diffraction. They contain cationic cluster units

- (20) *SHELXTL*, version 6.22; Bruker AXS, Inc.: Madison, WI, 2003.
- (21) Sheldrick, G. M. *SADABS, Program for Absorption Correction with the SMART System*; University of Göttingen: Göttingen, Germany, 1996.
- (22) Blatov, V. A. *Int. Union Crystallogr., Comm. Crystallogr. Comput. News.* **2006**, *7*, 4. (<http://www.iucr.org/iucr-top/comm/ccom/newsletters/>) <http://topos.ssu.samara.ru>.
- (23) Kniep, R.; Mootz, D.; Rabenau, A. Z. *Anorg. Allg. Chem.* **1976**, *422*, 17.

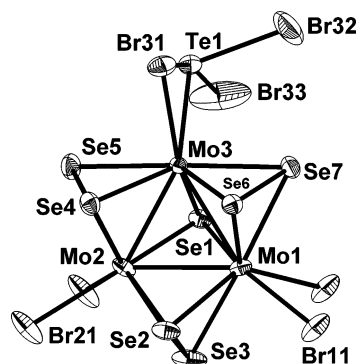


Figure 1. ORTEP drawing of the $[\text{Mo}_3\text{Se}_7(\text{TeBr}_3)\text{Br}_{4/2}]$ unit in **1**. All atoms are represented by the ADP ellipsoids at the 50% probability level.

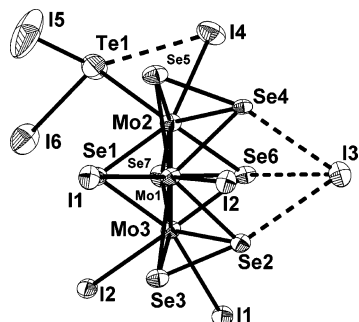


Figure 2. ORTEP drawing of the $[\text{Mo}_3\text{Se}_7(\text{TeI}_3)\text{I}_{4/2}]\text{I}$ unit in **2** showing the atom labeling scheme. All atoms are represented by the ADP ellipsoids at the 50% probability level.

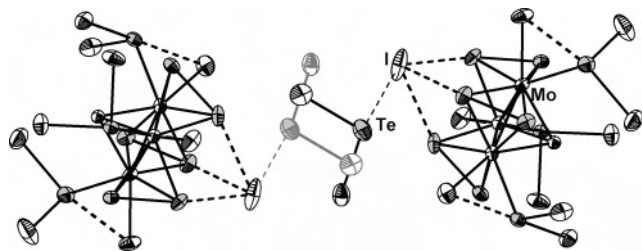


Figure 3. Superposition of $[\text{Mo}_3\text{Te}_7(\text{TeI}_3)_3]\text{TeI}_3$ and $[\text{Mo}_3\text{Te}_7(\text{TeI}_3)_3]\text{I}$ in **3** owing to disorder over the inversion center. Gray lines show the other position of the disordered anion TeI_3^- . Dashed lines correspond to $\text{Te}(\text{TeI}_3)\cdots\text{I}$ and $3\text{Te}_{\text{ax}}\cdots\text{I}$ (I^- and TeI_3^-) contacts.

$[\text{Mo}_3\text{Se}_7(\text{TeX}_3)\text{X}_{4/2}]^+$ ($\text{X} = \text{Br}$ (**1**), I (**2**)) which form zigzag chains, and a discrete cationic cluster $[\text{Mo}_3\text{Te}_7(\text{TeI}_3)_3]^+$ (in **3**). The counterions are $[\text{Te}_2\text{Br}_{10}]^{2-}$ in **1**, I^- in **2**, and I^- together with TeI_3^- in **3**. In this compound, the anions TeI_3^- and I^- are disordered over the inversion center so that the iodine atom belongs to both anions statistically. Despite disorder, we can unambiguously interpret the crystal packing in **3**, because every two disordered species can coexist only because the pair of $\{[\text{Mo}_3\text{Te}_7(\text{TeI}_3)_3]\text{TeI}_3\}$ and $\{[\text{Mo}_3\text{Te}_7(\text{TeI}_3)_3]\text{I}\}$ associate with no contradiction to both normal intermolecular distances and the stoichiometry of the compound. ORTEP drawings of $[\text{Mo}_3\text{Se}_7(\text{TeBr}_3)\text{Br}_{4/2}]^+$ in **1**, $\{[\text{Mo}_3\text{Se}_7(\text{TeI}_3)\text{I}_{4/2}]\text{I}\}$ in **2**, and $\{[\text{Mo}_3\text{Te}_7(\text{TeI}_3)_3]\text{I}\}$ and $\{[\text{Mo}_3\text{Te}_7(\text{TeI}_3)_3]\text{TeI}_3\}$ (in **3**) are shown in Figures 1–3, respectively.

In the $\text{Mo}_3\text{Q}_7^{4+}$ clusters, three Mo atoms define an equilateral triangle with an apical $\mu_3\text{-Q}$ atom ($\text{Mo}-\mu_3\text{-Se}$ is 2.47–2.48 Å) in **1** and **2**; $\text{Mo}-\mu_3\text{-Te}$ is about 2.66 Å in **3** (Table 2). The bridging Q_2 ligands are tilted in such a way

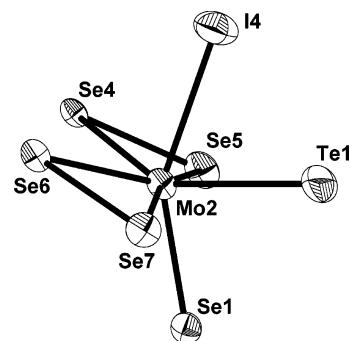


Figure 4. ORTEP drawing representing the local geometry around the Mo(2) atom in $\text{Mo}_3\text{Se}_7\text{TeI}_6$ (**2**). Atoms are represented by their ADP ellipsoids at the 50% probability level.

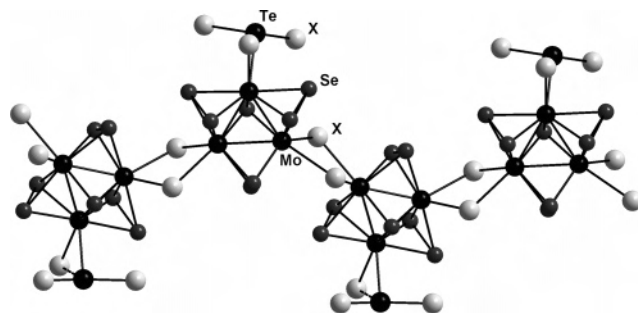


Figure 5. Fragment of crystal structure of **1** and **2**, viewed along the b axis.

that one Q atom lies in the same plane as the M_3 triangle (Q_{eq}) whereas the other is above the plane (Q_{ax}). The average $\text{Q}_{\text{eq}}-\text{Q}_{\text{ax}}$ distances in the Q_2 ligands are 2.307(5) Å for **1**, 2.40(3) Å for **2**, and 2.71(1) Å for **3** (Table 2). Thus, the Se–Se bond in **2** is significantly longer than that in **1** and in the rest of the $\text{Mo}_3\text{Se}_7^{4+}$ clusters.^{3,15c,24} The short contacts (less than the sum of the corresponding van der Waals radii) $3\text{Q}_{\text{ax}}\cdots\text{X}$, so-called “axial contacts”,⁷ result in the formation of the ion pairs $\{[\text{Mo}_3\text{Se}_7(\text{TeBr}_3)\text{Br}_{4/2}]^+\text{TeBr}_5^-\}$, $\{[\text{Mo}_3\text{Se}_7(\text{TeI}_3)\text{I}_{4/2}]^+\text{I}^-\}$, and $\{[\text{Mo}_3\text{Te}_7(\text{TeI}_3)_3]^+\text{I}^-\}$ (Table 2). Such contacts are typical of the $\text{M}_3\text{Q}_7^{4+}$ ($\text{M} = \text{Mo}, \text{W}$; $\text{Q} = \text{S}, \text{Se}, \text{Te}$) cluster cores.^{1,3,6,7,18,19}

Only one molybdenum atom in **1** and **2** and all three molybdenum atoms in **3** are coordinated to terminal TeX_3^- ligands in a bidentate (through both Te and one of the I) fashion, in a trans position with respect to the apical $\mu_3\text{-Q}$ atom being occupied by X and the cis position occupied by Te. Owing to this mode of coordination, the angles of $\text{Te}-\text{Mo}-\text{X}$ ($\text{X} = \text{Br}$, 65.2°; $\text{X} = \text{I}$, 67.5° (compound **2**), 66.0° (compound **3**)) are similar to those of $\text{Mo}_3\text{Te}_{10}\text{I}_{10}$ (65.3°) and smaller by 10–15° compared with the angles $\text{X}-\text{Mo}-\text{X}$ of $\text{Mo}_3\text{Q}_7\text{X}_6^{2-}$ ($\text{Q} = \text{S}, \text{Se}$). The tellurium atoms of the TeX_3^- ligands have distorted trigonal-bipyramidal geometry as predicted from VSEPR model consideration. The distortion is caused by coordination to Mo (in equatorial position) and by the stereochemically active lone pair, also in the equatorial position. The distortion, as measured by

(24) (a) Sokolov, M. N.; Gushchin, A. L.; Naumov, D. Yu.; Gerasko, O. A.; Fedin, V. P. *Inorg. Chem.* **2005**, *44*, 2431. (b) Berau, V.; Ibers, J. A. C. *R. Acad. Sci. Ser. IIc: Chim.* **2000**, *3*, 123. (c) Almond, M. J.; Drew, M. G. B.; Redman, H.; Rice, D. A. *Polyhedron* **2000**, *19*, 2127.

Table 2. Characteristic Bond Lengths (Å) and Angles (deg) for **1–3** (min–max, Average)

	1 (Q = Se, X = Br)	2 (Q = Se, X = I)	3 (Q = Te, X = I)
Cluster Core			
Mo–Mo	2.7567(13)–2.7644(12), 2.761[4]	2.759(3)–2.783(3), 2.77[1]	2.8472(19)–2.8553(19), 2.851[4]
Mo–Q _{eq}	2.5965(14)–2.6224(17), 2.61[1]	2.616(4)–2.649(4), 2.63[1]	2.7772(18)–2.8491(17), 2.82[3]
Mo–Q _{ax}	2.5235(15)–2.5467(15), 2.563[9]	2.552(3)–2.643(4), 2.60[4]	2.7305(18)–2.7613(16), 2.75[1]
Mo–μ ₃ -Q	2.4633(14)–2.4807(15), 2.474[9]	2.482(4)–2.486(4), 2.482[5]	2.6571(17)–2.6689(16), 2.662[6]
Ligands			
Q _{eq} –Q _{ax} (Q ₂ ²⁻)	2.3006(17)–2.3101(18), 2.307[5]	2.365(4)–2.430(4), 2.40[3]	2.7021(17)–2.7248(16), 2.71[1]
Mo–Te (TeX ₃ ⁻)	2.8090(12)	2.769(3)	2.7714(17)–2.7882(17), 2.781[9]
Mo–X (TeX ₃ ⁻)	2.611(15)	2.846(3)	2.8652(16)–2.8812(16), 2.876[9]
Te–X	2.4723(17), 2.517(2)	2.755(5), 2.769(4)	2.7539(17)–2.8130(17), 2.78[2]
Te···X (MoTeX ring)	2.9430(16)	3.121(3)	3.0569(17)–3.1013(16), 3.08[2]
Nonvalent Contacts			
Q _{ax} ···X ⁻	3.0485(18)–3.3282(18), 3.2[1]	3.169(3)–3.212(3), 3.19[2]	3.248(2)–3.450(2), 3.3[1]
Q _{eq} ···X ⁻	3.6215(16)	3.407(4)	no
Q _{ax} –Q _{eq} ···X ⁻	161.90(6)	166.62(14)	no

the angle between two halides in the axial position, increases in the order **1** (162.4°) < **3** (157.3°) < **2** (143.6°). The Te–X distances in the MoTeX ring are much longer in comparison with the bond lengths (Table 2) to the uncoordinated halogen atoms of the TeX₃⁻ ligands. Accordingly, the coordination to the Mo atom leads to some redistribution of the bond distances in TeI₃⁻. In noncoordinated TeI₃⁻ in **3**, two Te–I bond distances of 2.719(6) and 2.725(5) Å are slightly shorter, whereas the third distance of 3.171(5) Å is longer than that in the coordinated TeI₃⁻ (Table 2). However, the latter value may also be affected by disorder if one takes into account the shape of the atomic displacement parameter (ADP) ellipsoid of the iodine atom (Figure 3), but the Te–I bond length of the MoTeI triangle (3.121(3) Å) is comparable to the Te–I bond lengths of 3.06 and 3.22 Å in the central four-membered Te₂I₂ ring of the Te₂I₆²⁻ anion (Te₂Br₆²⁻ is unknown).²⁵ Alternatively, the coordination around Mo can be described as being provided by two separate ligands X⁻ and neutral TeX₂, with a secondary interaction between them resulting mainly from geometrical constraints. The same ambiguity is present in the description of the coordination in cuboidal [Re₄Te₄Br₈(TeBr₂)₄], where the choice is between the planar TeBr₄²⁻ ligand, coordinated in an “allylic”, η³ fashion, and the neutral TeBr₂ molecule (Te–Br 2.51–2.54 Å), weakly bound to two coordinated bromines (Te···Br 2.92–2.96 Å).²⁶ A very similar situation (η³-TeBr₄²⁻ vs TeBr₂ + 2Br⁻) is found in [Re₂(μ-TeBr)₂(μ-Te)₂(TeBr₂)₂-Br₄].²⁷ A choice between η³-coordinated Te₂I₆²⁻ and a set of two TeI₂ and two I⁻ atoms is possible in [Nb₂(Q₂)₂(Te₂I₆)₂] (Q = Se, Te).²⁵ Even in [Re₆Te₈(TeBr₂)₆]Br₂, which appears as more genuine complexes of TeBr₂, anionic Br⁻ atoms

weakly interact with three coordinated TeBr₂ ligands (Te···Br 3.17 Å).²⁸ In [Re₆Te₈(TeI₂)₆]I₂, the shortest I⁻···Te contact is 3.45 Å, and the description of the coordinated ligand as TeI₂ is the most appropriate here.²⁹

As discussed in ref 16, if metal–metal interactions are ignored, each molybdenum atom can be considered hepta-coordinated. The Mo(Q₂)₂ and Mo(μ₃-Q)XTe units are both nearly planar and mutually perpendicular. This geometrical picture can be even further simplified by imagining bonding to the midpoint of the Q–Q bond, in which case the resulting geometry around the molybdenum atoms is distorted trigonal bipyramidal, as shown in Figure 4.

The four halogen atoms at two molybdenum atoms in **1** and **2** link the cluster units into extended zigzag chains $\frac{1}{2}[\text{Mo}_3\text{Se}_7(\text{TeX}_3)\text{X}_{4/2}]^+$, where μ₃-Se atoms of cluster units are directed alternatively “up” and “down” (Figure 5). Thus, the structure of **2** can easily be derived from the structures of $\frac{1}{2}[\text{Mo}_3\text{S}_7\text{Cl}_2\text{Cl}_{4/2}]$ and $\frac{1}{2}[\text{W}_3\text{S}_7\text{Br}_2\text{Br}_{4/2}]$ by substituting the two terminal, nonbridging halide ligands with the bidentate anionic TeI₃⁻ ligand, pushing one of the I⁻ atoms into the cavity formed by the three axial Se atoms (Se_{ax}) to maintain electroneutrality. These 3Se_{ax}···I⁻ (axial) contacts are much shorter (Table 2) than those found in an anionic cluster complex, {[Mo₃Se₇(CN)₆]I³⁻} (3.45 Å),³ most probably due to the favorable electrostatic factor. Contacts of similar lengths, interpreted as chemical bonds, were found in polymeric dithiocarbamates *catena*-(R₂NCS₂SeI)_n (3.1–3.2 Å)³⁰ and in three-coordinate PhSeI(PPh₃) (3.26 Å).³¹ This

(25) (a) Fedin, V. P.; Fedorov, V. E.; Imoto, H.; Saito, T. *Polyhedron* **1997**, *16*, 995. (b) Leist, A.; Tremel, W. *Angew. Chem.* **1993**, *105*, 1798.(26) Schulz Lang, E.; Abram, U.; Straehle, J. Z. *Anorg. Allg. Chem.* **1996**, *622*, 251.(27) Beck, J.; Mueller-Buschbaum, H. *Eur. J. Inorg. Chem.* **1999**, 839.(28) Mironov, Yu. V.; Pell, M. A.; Ibers, J. A. *Inorg. Chem.* **1995**, *35*, 2709.(29) Fedin, V. P.; Fedorov, V. E.; Imoto, H.; Saito, T. *Polyhedron* **1997**, *16*, 1615.(30) (a) Bigoli, F.; Leporati, E.; Pellinghelli, M. A.; Crisponi, G.; Deplano, P.; Trogu, E. F. *J. Chem. Soc., Dalton Trans.* **1983**, 1763. (b) Rajashree, S.; Kumar, P. K.; Aravamudan, G.; Udupa, M. R.; Sivakumar, K.; Fun, H.-K. *Acta Crystallogr., Sect. C.* **1999**, *55*, 1320.

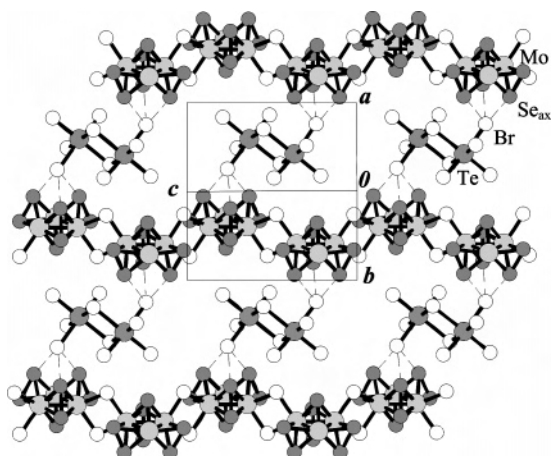


Figure 6. Layers built on $3\text{Se}_{\text{ax}}\cdots\text{Br}$ ($\text{Te}_2\text{Br}_{10}^{2-}$) axial contacts (dashed lines) in **1**. TeBr_3^- ligands are not shown for clarity.

is of course still much longer than the “normal” Se–I bond length, found in ArSeI (2.53 Å).³²

The situation in **1** is similar, except that the outer-sphere bromide belongs to the $[\text{Te}_2\text{Br}_{10}]^{2-}$ anions (Figure 6). The Te–Br bond lengths to the terminal bromine ligands in $[\text{Te}_2\text{Br}_{10}]^{2-}$ are within the normal bonding range (av 2.538³ Å), whereas distances to the bridging ligands are much longer (2.935(4) and 2.967(3) Å). The observed asymmetry in these bonds was as found earlier in $[(\text{C}_2\text{H}_5)_4\text{N}]_2[\text{Te}_2\text{Br}_{10}]$ (Te–Br₁ = 2.566–2.569 and 2.671–2.689 Å; Te–μ₂-Br = 2.920–2.930 Å) and also for $[\text{Te}_2\text{Cl}_{10}]^{2-}$ and $[\text{Te}_2\text{I}_{10}]^{2-}$ salts.³³ The $3\text{Se}_{\text{ax}}\cdots\text{Br}^-$ contacts (Table 2) nearly fall in the range found for $\{[\text{Mo}_3\text{Se}_7(\text{C}_2\text{O}_4)_3]_2\text{Br}\}^{5-}$.^{24a}

Curiously, in $[\text{Fe}_2(\text{CO})_6(\text{TeCl}_2)_2\text{Cl}]_2[\text{Te}_2\text{Cl}_{10}]$ $[\text{Te}_2\text{Cl}_{10}]^{2-}$ also participates in secondary bonding between two $[\text{Fe}_2(\text{CO})_6(\text{TeCl}_2)_2\text{Cl}]^+$ cations through weak Te \cdots Cl contacts (2.859(2) Å).³⁴

Crystal Packing in 1–3. The analysis of the crystal structures of various $\{\text{M}_3\text{Q}_7\}$ derivatives shows that nonvalent interactions involving both equatorial (Q_{eq}) and axial (Q_{ax}) chalcogen atoms play a key role in the crystal packing.⁷ The axial $3\text{Q}_{\text{ax}}\cdots\text{Y}$ contacts control the mutual arrangement of cluster complexes and counterions. We found these contacts in all $\{\text{M}_3\text{Q}_7\}$ derivatives, except three, namely, $(\text{AsPh}_4)_2[\text{Mo}_3\text{S}_7(\text{S}_2)_3]\cdot 2\text{CH}_3\text{CN}$, $(\text{NH}_4)_4[\text{Mo}_3\text{S}_{11.72}\text{Se}_{1.28}]_2\cdot (\text{Se}_{12})$, and $(\text{endo-H}_2)[\text{Mo}_3\text{Se}_7(\text{Se}_2)_3]$.³⁵ Additional equatorial contacts^{7b} involve the Q_{eq} atom and an external atom that can belong to the counterion, neighbor-cluster complex, etc. These equatorial contacts occur very rarely when $\text{Q} = \text{S}$, more frequently when $\text{Q} = \text{Se}$, and very frequently when $\text{Q} = \text{Te}$.^{7b} They lead to the formation of chains, layers, and

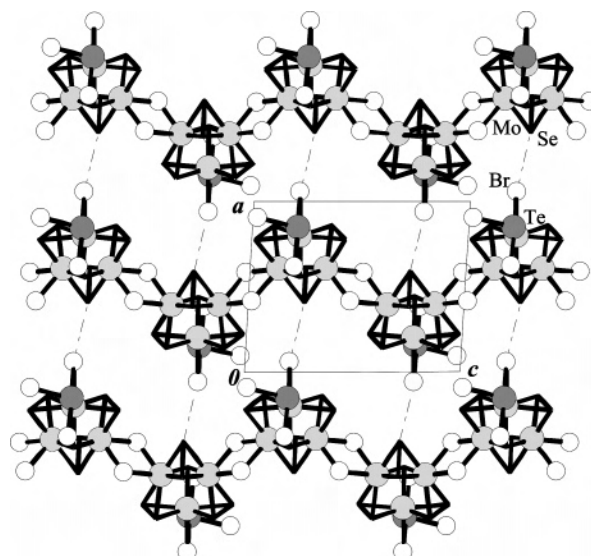


Figure 7. Planar layer formed by nonvalent equatorial contacts $\text{Se}_{\text{ax}}\cdots\text{Br}$ of 3.62 Å in **1** (dashed lines). Mo–Mo bonds are hidden for clarity.

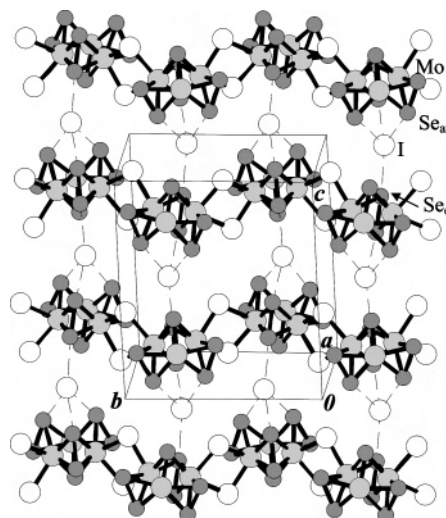


Figure 8. Layer in **2** built on both $3\text{Se}_{\text{ax}}\cdots\text{I}$ axial and $\text{Se}_{\text{ax}}\text{--}\text{Se}_{\text{eq}}\cdots\text{I}$ equatorial contacts (dashed lines).

even three-dimensional (3D) frameworks. In **1**, each $\{\text{Mo}_3\text{Se}_7\}$ cluster unit forms three $\text{Se}_{\text{ax}}\cdots\text{Br}$ axial contacts (Table 2) with the terminal bromine atom of the $\text{Te}_2\text{Br}_{10}^{2-}$ anion. Another terminal bromine atom of the same anion participates in similar contacts with the Se_{ax} atoms of the nearest chain. These axial contacts join the chains into corrugated [110] layers (Figure 6). At the same time, Se_{eq} forms equatorial nonvalent contacts that involve the Br atoms of a TeBr_3^- ligand belonging to another chain so that a 3D supramolecular framework forms (Figure 7).

In **2**, the resulting net of axial $3\text{Se}_{\text{ax}}\cdots\text{I}$ and equatorial $\text{Se}_{\text{ax}}\text{--}\text{Se}_{\text{eq}}\cdots\text{I}^-$ contacts has lower dimensionality. Each cluster unit forms three axial contacts with the iodide anion, which, in turn, is connected with Se_{eq} of the neighboring chain. The contacts of both types join the cluster chains into corrugated layers in [100] (Figure 8). Due to steric reasons in both **1** and **2**, only the Se_{eq} atom most remote from the coordinated TeX_3^- can form short equatorial contacts.

(31) Boyle, P. D.; Godfrey, S. M.; McAuliffe, C. A.; Pritchard, R. G.; Sheffield, J. M. *Chem. Commun.* **1999**, 2159.

(32) du Mont, W. W.; Rubiniok, S.; Peters, K.; von Schnering, H.-G. *Angew. Chem., Int. Ed.* **1987**, 26, 780.

(33) Krebs, B. *Nova Acta Leopold.* **1985**, 59, 131.

(34) Eveland, J. R.; Whitmire, K. H. *Angew. Chem., Int. Ed. Engl.* **1996**, 35, 741.

(35) (a) Muller, A.; Wittneben, V.; Krickemeyer, E.; Bogge, H.; Lenke, M. *Z. Anorg. Allg. Chem.* **1991**, 605, 175. (b) Stevens, R. A.; Raymond, C. C.; Dorhout, P. K. *Angew. Chem., Int. Ed. Engl.* **1995**, 34, 2509. (c) Ying, W.; Jie-Sheng, C.; Hong-Ming, Y.; Zhan, S.; Shao-Fang, Y.; Wei, C. *Chin. J. Chem.* **2001**, 19, 681.

Accordingly, no such equatorial contacts are found in **3**, where all three Mo atoms are coordinated to bulky TeI_3^- ligands. In this compound, each neutral species, $[\text{Mo}_3\text{Te}_7(\text{TeI}_3)_3]\text{TeI}_3$ or $[\text{Mo}_3\text{Te}_7(\text{TeI}_3)_3]\text{I}$, is surrounded by 13 neighbors, 6 of the same sort and 7 of the other. The “ordered” crystal packing, where all pairs of different species are in the same orientation, may also be described as two interpenetrating sublattices consisting of a one-sort species with the topology of face-centered-cubic packing.

In conclusion, high-temperature reactions in the Mo–Se–Te–I system lead to incorporation of Se in the cluster core, while Te is oxidized into Te(II) species that are stabilized by coordination to the cluster. In the Mo–Se–Te–Br system, the situation is similar—Se enters the core, while Te goes into Te(II) and even Te(IV), which play an important role in the building of the crystal lattice. TeBr_3^- (observed

for the first time) is stabilized by coordination. Noncoordinated TeI_3^- was also observed by the first time and is stabilized by nonvalent interactions.

Acknowledgment. The work was supported by the Russian Foundation for Basic Research (Grant 05-03-32126), the Haldor Topsøe Foundation (A.L.G.), and the Presidium of the Siberian Branch of the Russian Academy of Sciences (Lavrentyev Grant for Young Scientists to E.V.P.). M.N.S. is grateful for the Presidential Grant MD 7072.2006.3. We thank Prof. V. A. Blatov for providing the *TOPOS 4.0 Professional* software.

Supporting Information Available: CIF files for structures **1–3**. This material is available free of charge via the Internet at <http://pubs.acs.org>.

IC0700553